A&A 426, 247–252 (2004)
DOI: 10.1051/0004-6361:20034068

Astronomy & Astrophysics

HD 173977: An ellipsoidal δ Scuti star variable[⋆,⋆⋆]

E. Chapellier[1], P. Mathias[1], R. Garrido[2], J.-M. Le Contel[1], J.-P. Sareyan[1], I. Ribas[3], L. Parrao[4], A. Moya[2], J. H. Peña[4], and M. Alvarez[5]

[1] Observatoire de la Côte d'Azur, Département GEMINI – UMR 6203, BP 4229, 06304 Nice Cedex 4, France
e-mail: [eric;mathias]@obs-nice.fr
[2] Instituto de Astrofisica de Andalucia, Apt. 3004, 18080 Granada, Spain
[3] Departamento de Astronomia y Meteorologia, Universitat de Barcelona, 08028 Barcelona, Spain
[4] Instituto de Astronomia de la UNAM, Ap. P. 877, Ensenada, BC, Mexico
[5] Instituto de Astronomia, Universidad Nacional Autonoma de Mexico, Apdo. Postal 70-264, Mexico DF 04510, Mexico

Received 10 July 2003 / Accepted 23 June 2004

Abstract. We present spectroscopic and photometric observations of the star HD 173977. It appears that the star is part of a double line binary system, with a period of 1.801 d, corresponding to twice the period of the photometric variations. Hence the star is an ellipsoidal variable. The system is probably synchronized. The physical parameters of both components were derived through two independant methods, one based on evolutionary tracks, the other being the result of the behaviour of light curves in a close binary system. After removing the ellipsoidal variations, 3 frequencies are detected in the photometric data: 8.56, 14.51 and 16.42 d^{-1}, while 2 additional frequencies are also possible: 10.96 and 12.11 d^{-1}. In accordance with its position in the HR diagram, the primary component of HD 173977 should be considered as a δ Scuti star and no longer as a γ Doradus star. In addition, HD 173844, used as a check star, is discovered variable with a 15.79 d^{-1} frequency and is classified as a δ Scuti star.

Key words. stars: binaries: general – stars: oscillations – techniques: photometric – techniques: spectroscopic – stars: variables: δ Sct

1. Introduction

HD 173977 (HN Dra, HIP 91983, F1, B=8.43, V=8.11) was discovered to be variable by the Hipparcos group (ESA, 1997) with a period of 0.9 d. It was then classified as "a prime γ Doradus candidate" by Handler (1999) who derived two periods, namely 0.900 and 1.327 d from the same photometric Hipparcos data. Fekel et al. (2003) obtained 2 spectra and found large variations both in line profile and in radial velocity, which led them to classify the star as a single line spectroscopic binary. This star was included in an observational photometric and spectroscopic campaign (Mathias et al., 2004) to compare its photometric and spectroscopic periods and to determine its pulsational modes from the line profile and radial velocity variations. A rapid inspection of the first spectra showed that two components were present, so we decided to study this star in more detail to disentangle binary motions and pulsational variations.

We present in Sect. 2 the spectroscopic and photometric observations, while Sect. 3 deals with the orbital parameters and the pulsation behaviour. A short discussion is given in Sect. 4.

⋆ Based on observations obtained at the Observatoire de Haute-Provence.

⋆⋆ Spectroscopic and photometric data are only available in electronic form at the CDS via anonymous ftp to
cdsarc.u-strasbg.fr (130.79.128.5) or via
http://cdsweb.u-strasbg.fr/cgi-bin/qcat?J/A+A/426/247

2. Observations

Spectroscopic and photometric data are available at the CDS.

2.1. Spectroscopy

Spectroscopic observations were obtained at the Observatoire de Haute-Provence (France) with the AURELIE spectrograph attached to the Coudé focus of the 1.52 m telescope. The spectral resolution was $\lambda/\Delta\lambda = 55\,000$ in a domain of about 70 Å, centered on the unblended Fe II and Ti II lines at respectively 4501 and 4508 Å. With a typical exposure time of 1 h, the average *S/N* ratio was about 190. We obtained 35 spectra spread over 416 days from August 2001 to October 2002. Standard reductions were performed with the IRAF package and radial velocity measurements were made using a Gaussian fit to the observed line profiles of the lines cited above.

2.2. Photometry

Photometric observations were obtained in August and September 2001 at the 0.9 photometric telescope of the Sierra Nevada Observatory (Spain) and at the 1.5 m telescope at San Pedro Martir Observatory (Mexico). Both sites have a 4-channel multicolor Strömgren spectro-photometer. We obtained 69 measurements spread over 48 days in the four u, v, b, y filters. We used HD 173663 (A2, $V = 8.43$) and HD 173844

(A2, $V = 8.70$) as comparison stars. HD 173844 turned out to be a δ Scuti star with a main frequency of $15.79\,d^{-1}$ and an associated amplitude of 4.6 mmag in v. Thus reductions were made with respect to HD 173663, and carefully done in order to mix Granada and San Pedro Martir data.

We obtained another more homogeneous data set from San Pedro Martir in 2002, representing 156 measurements over 14 consecutive nights.

Note that in the following, the data obtained in the u-filter have not been considered because of a too large dispersion.

3. Results

3.1. The binary system

Spectra clearly show the presence of two line systems, so HD 173977 should be classified as a double line spectroscopic binary. The large line asymmetries described by Fekel et al. (2003) are certainly due to the presence of the weak lines of the companion, the residual flux of which are about 1/3 that of the main component. We measured the lines of the components using a Gaussian fit to both Ti II and Fe II lines. The average of the derived velocities are listed in Table 1. We also considered the two velocity values given by Fekel et al. (2003) to derive the parameters of the binary orbit that are provided in Table 2. This orbit is represented, for both components, in Fig. 1.

The 0.9 d period provided by the Hipparcos team (ESA, 1997) corresponds to half the orbital period. A sinusoidal fit performed on the Hipparcos data gives an amplitude of 0.037 mag which represents about 75% of the variance. The 0.9 d period is also found in our Strömgren photometric data the results of the sine-fit are reported in Table 3. Amplitudes in the different filters, although close to each other, are not equivalent. This is certainly directly linked to the shape of the star, with low temperatures at both ends and enhanced temperatures in the narrow region. The v-filter data, phased with the orbital period, are plotted in the bottom panel of Fig. 1. The phase origin has been arbitrarily fixed to the time of light minimum.

From our data set, combined with the Hipparcos data, we derived the following ephemeris for the photometric variations:

$$L_{\max} = \mathrm{HJD}(2\,448\,000.858 \pm 0.029) + (0\overset{d}{.}9003756 \pm 0\overset{d}{.}0000093)\,E$$

where the error bars represent 3σ, σ being computed following Montgomery & O'Donoghue (1999).

3.2. Pulsation

After prewhitening the data for the ellipsoidal variations, we looked for frequencies which could arise from pulsations. The two data sets (2001 and 2002) were analysed separately with the following method. The main peak was obtained from a Fourier analysis using Period 98 (Sperl 1998) and Vanicek's program (1971). The peaks are searched for up to frequencies lower than $30\,d^{-1}$, since the Nyquist frequency provided by Period 98 is $71\,d^{-1}$. The frequency corresponding to this main peak was then refined by a sinusoidal adjustment. We retained the frequency having the largest amplitude and the smallest residuals. After prewhitening the data for the determined frequency, the same analysis was performed (i.e. main peaks, sinusoidal adjustment with all frequencies) as many times as necessary until no dominant peaks could be determined. Vanicek's method iterates until the simultaneous removal of the corresponding frequencies at each step is not statistically significant.

Table 1. The first column displays the Heliocentric Julian Day for mid-exposure, while the two next columns list the velocity values [km s^{-1}] corresponding to the average between those of the Fe II and Ti II lines associated with each component. Only the velocities corresponding to the best spectra (high *S/N* ratio, no cosmics within the profiles, 2 components well fitted) are given.

HJD - 2 452 000	Component 1	Component 2
133.3791	–82.4	96.1
150.4362	51.5	–92.8
406.6092	69.2	–106.1
407.3550	–100.4	129.8
407.6226	–49.8	54.8
414.5418	–103.3	128.9
415.5364	82.2	–132.9
416.4941	–79.9	105.1
418.5493	–5.1	–1.8
420.5513	51.6	–96.0
422.5458	86.9	–140.5
423.4181	–101.0	125.2
423.5788	–97.0	128.9
424.5815	76.5	–116.9
425.3562	–101.6	131.6
425.5879	–58.9	73.9
428.5908	–53.7	54.7
429.4655	25.6	–
447.5395	44.8	–93.4
450.3908	–98.4	118.4
499.4842	–45.2	–
503.3767	48.7	–96.6
505.3981	89.7	–149.0
506.3479	–102.0	137.2
535.3225	–78.6	–
535.3667	–73.3	–
541.3591	82.5	–
543.3545	86.8	–
549.3394	–79.3	97.1

Table 2. Parameters of the binary orbit. Note that subscripts 1 and 2 refer respectively to the primary and the secondary stars of HD 173977. The final rms of the residuals, after iteration, is 3.23 km s^{-1}.

P	=	1.800745 ± 0.000020 d
T_0	=	2452106.73 ± 0.28 d
e	=	0.0060 ± 0.0054
γ	=	-6.69 ± 0.45 km s^{-1}
K_1	=	96.70 ± 0.77 km s^{-1}
ω_1	=	43 ± 57^o
$a_1 \sin i$	=	$(2.39 \pm 0.02)10^6$ km
$M_1 \sin^3 i$	=	$1.471 \pm 0.009\,M_\odot$
K_2	=	140.21 ± 0.88 km s^{-1}
ω_2	=	223 ± 57^o
$a_2 \sin i$	=	$(3.47 \pm 0.02)10^6$ km
$M_2 \sin^3 i$	=	$1.015 \pm 0.007\,M_\odot$

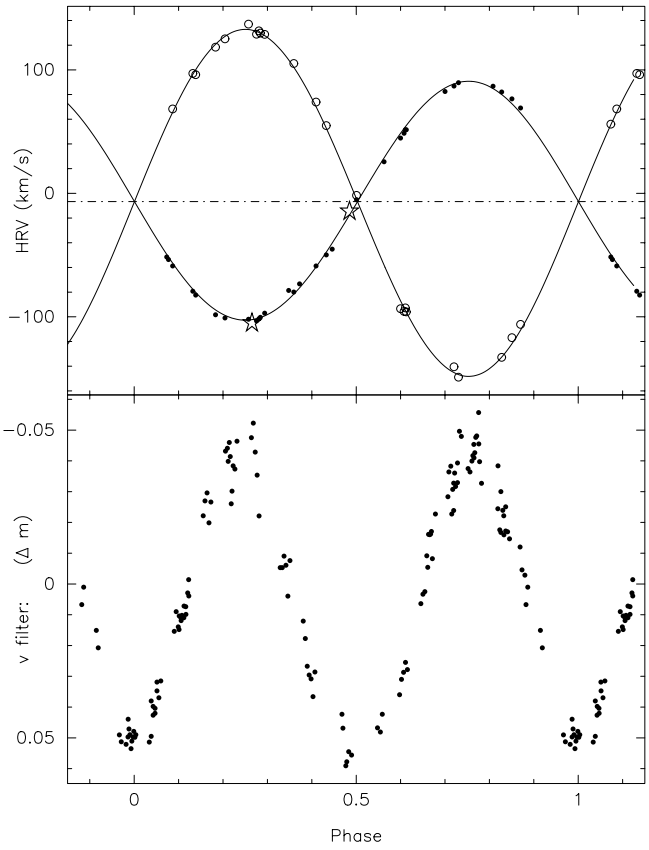

Fig. 1. *Top*: fit of the orbits of the HD 173977 primary (dots) and secondary (open circles). The two star symbols represent the measurements of Fekel et al. (2003). The dot-dash line represents the heliocentric velocity of the system. *Bottom*: v-filter photometric differential magnitudes data phased with the orbital period. Note that the pulsation frequencies have been removed (see Sect. 3.2).

Table 3. Results of a sine-fit performed to the Strömgren photometric data for the ellipsoidal period. The right part of the table shows the values once the pulsation frequencies have been removed. Amplitudes and rms are in mmag.

Filter	A	rms	A	rms
v	45.7 ± 3.8	10.8	48.6 ± 1.5	4.1
b	41.6 ± 3.2	9.0	43.9 ± 1.4	3.8
y	36.0 ± 2.6	7.3	38.1 ± 1.2	3.5

The successive Fourier spectra for the v, b and y filters for the two data sets are shown in Figs. 2–4. The data resulting from the sinusoidal adjustments for the detected pulsation frequencies are given in Tables 4 and 5.

2001 data: a main frequency at $8.557\,\mathrm{d}^{-1}$ is present in the three filters (Fig. 2). The sinusoidal adjustment leads to the values listed in Table 4. After prewhitening for this frequency, no other significant peak is present.

2002 data: the same main frequency ($8.56\,\mathrm{d}^{-1}$) is present in the three filters (Fig. 3). After prewhitening the data for this frequency, two low frequency peaks corresponding to the orbital frequency ($f_{\mathrm{orb}} = 0.55\,\mathrm{d}^{-1}$, with $A_v = 5.9$ mmag, $A_b = 4.8$ mmag and $A_y = 3.8$ mmag) and to its $1.67\,\mathrm{d}^{-1}$ harmonic ($3f_{\mathrm{orb}}$, with $A_v = 3.5$ mmag, $A_b = 2.9$ mmag and

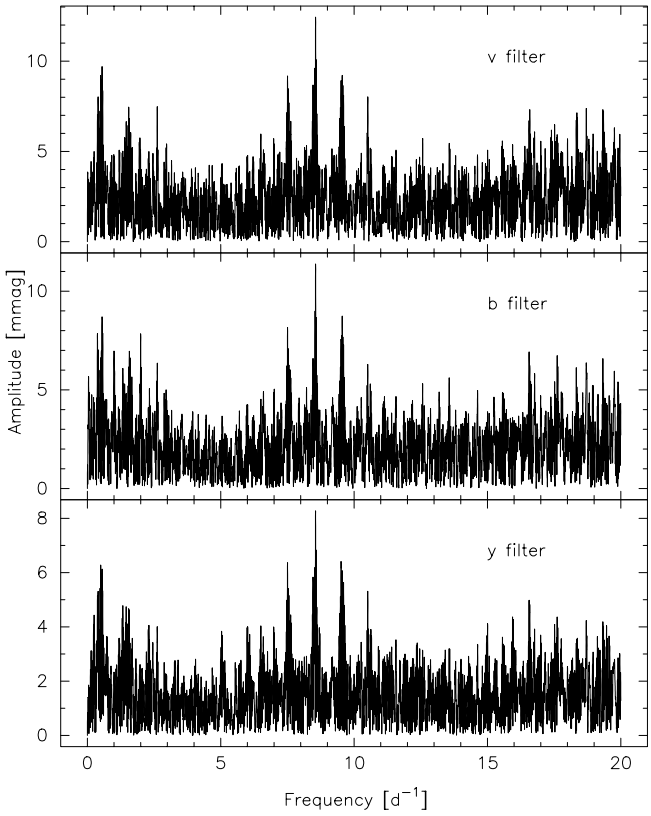

Fig. 2. Amplitude spectra in the different filters for the 2001 data.

$A_y = 2.6$ mmag) dominate the power spectra. This is not surprising as the photometric light curves due to the orbital movement are not sinusoidal (Fig. 1). This phenomenon, which does not deal with the pulsation, will be discussed in Sect. 4.1. Thus, the data are prewhitened for these two frequencies and then analysed to derive the pulsation frequencies. In the three filters a frequency at $14.51\,\mathrm{d}^{-1}$ is dominant (Fig. 3). This frequency could be an alias of the main frequency f_1. However, the Fourier spectrum presents peaks, centered on $8.56\,\mathrm{d}^{-1}$, that are in the range $[5.56;12.56]\,\mathrm{d}^{-1}$. After $12.56\,\mathrm{d}^{-1}$, the Fourier spectrum reaches the noise limit. After prewhitening for the $8.56\,\mathrm{d}^{-1}$ frequency, the peak series centered on 14.51 c/d is not affected. Therefore, it seems that these two frequencies are independent.

After prewhitening for this new frequency, no peak dominates the frequency power spectra. However in the v and b filters, two sets of frequencies centred at $11\,\mathrm{d}^{-1}$ and preferably at $16.4\,\mathrm{d}^{-1}$ are detected, with a main peak at $16.42\,\mathrm{d}^{-1}$. In the y filter the one day alias frequency peak at $15.43\,\mathrm{d}^{-1}$ appears slightly higher than the $16.42\,\mathrm{d}^{-1}$ one ($a = 1.715$ mmag, residuals 3.372 against 1.683 mmag and 3.377). The difference is so weak that we retained the $16.42\,\mathrm{d}^{-1}$ frequency value for the three filters (in δ Scuti stars the amplitude in the y filter is lower that in the v and b ones). Note that since the shortest interval between 2 observational points is 0.008 d, this frequency covers 8 mean measures. When the data are prewhitened for this new frequency, a series of very closed double peaks appears centred around $11\,\mathrm{d}^{-1}$. Again, in the v and b filters, a main peak at $10.96\,\mathrm{d}^{-1}$ is detected with amplitudes of 2.3 and 2.0 mmag

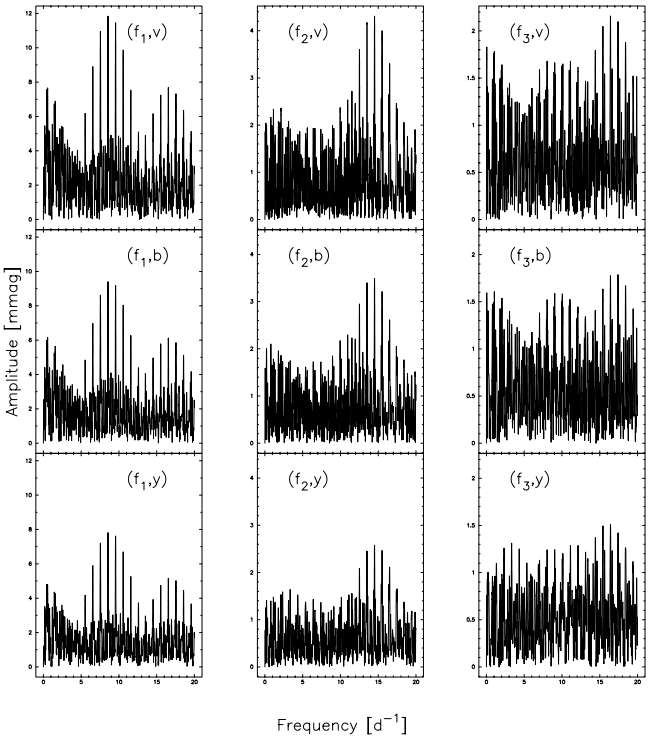

Fig. 3. Amplitude spectra in the different filters for the 2002 data showing the 3 first frequencies. The dominant frequency together with the considered filter are given in each panel.

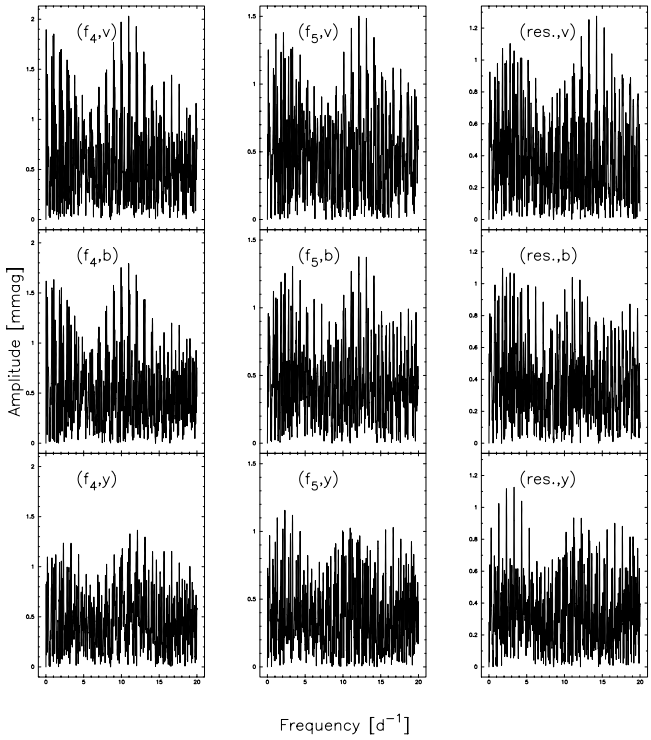

Fig. 4. Amplitude spectra in the different filters for the 2002 data. Last column shows the residuals after prewhitening for the 5 frequencies.

respectively. Conversely, in the y filter, the second component of the double peak is dominant at $12.12\,\mathrm{d}^{-1}$ with 1.6 mmag.

When we prewhitened the v and b filter data for the $10.96\,\mathrm{d}^{-1}$ frequency and the y filter data for the $12.12\,\mathrm{d}^{-1}$ frequency, we found a peak at $12.11\,\mathrm{d}^{-1}$ for both v and b filters (respective amplitudes of $a = 1.8$ and 1.6 mmag) and $10.96\,\mathrm{d}^{-1}$ ($A = 1.2$ mmag) for the y filter. Thus in the three filters, we actually detected the two $10.96\,\mathrm{d}^{-1}$ and $12.11\,\mathrm{d}^{-1}$ frequencies although the order is different in the y filter.

Applying the statistical test of Scargle (1982), we find a detection threshold in the v, b and y filters equal to 2.12, 2.01 and 1.76 mmag. These thresholds are calculated for a confidence level of 99%. A comparison with the obtained amplitudes for the 8.56, 14.51 and $16.42\,\mathrm{d}^{-1}$ frequencies shows that they are above the detection thresholds. Conversely, the amplitudes corresponding to the 10.96 and $12.11\,\mathrm{d}^{-1}$ frequencies are close to (in the v and b filters) or below (in the y filter) the detection threshold. In addition, the fact that these frequencies form a system of double peaks increases the possible existence of aliases and so induces possible errors in the identification of the main peaks.

As a conclusion, we consider the 8.56, 14.51 and $16.42\,\mathrm{d}^{-1}$ frequencies as pulsation frequencies present in HD 173977. Finally a sinusoidal adjustment of the data with the five frequencies simultaneously has been performed. The results are listed in Table 5 where the error bars have been determined using the method of Montgomery & O'Donoghue (1999) for a 3σ-value. Finally, we consider that HD 173977 pulsates with three confirmed and two possible frequencies.

Table 4. Results of the Fourier analysis performed on the 2001 photometric data, prewhithened for the ellipsoidal variations. For the different filters are given the dominant frequency f [d^{-1}], the corresponding amplitude A [mmag] and the phase φ [period fraction] (with respect to the first data point [HJD 2 452 124.3616]). The residuals for the v, b and y filters are respectively 8.1, 7.6 and 5.7 mmag.

Filter	f	A	φ
v	8.5574	12.1	0.949
	±22	±2.8	±36
b	8.5575	10.9	0.959
	±23	±2.6	±38
y	8.5560	7.6	0.017
	±25	±1.9	±40

In order to see if these frequencies are present also in the Hipparcos data, we re-analyzed them using the same procedure. We confirm that the second frequency provided by Handler (1999) is found in the Hipparcos data. This frequency, $0.75365\,\mathrm{d}^{-1}$, has an amplitude of 9.2 mmag. However, if still present in 2001–2002, this period would have been easily detected in our data, but definitively no peak is present. On the other hand, no signature of our 4 detected pulsational frequencies is present in the periodogram, which is certainly due to the Hipparcos data sampling which prevents the detection of high frequencies.

We did not succeed in deriving any frequency in the spectroscopic data set prewhitened for the orbital period, due to a bad sampling because the exposure time represents at least 35% of the period. However, no line profile variations usually attributed to γ Doradus variables are observed.

Table 5. Results of the Fourier analysis performed on the 2002 photometric data, prewhitened for the ellipsoidal variations. For the different filters are given the detected frequencies f [d^{-1}], the corresponding amplitude A [mmag] and the phase φ [period fraction] (with respect to the first data point [HJD 2 452 498.65555]). The residuals for the v, b and y filters are respectively 3.1, 2.9 and 2.5 mmag.

	v-filter			b-filter			y-filter		
	f	A	φ	f	A	φ	f	A	φ
f_1	8.5592	10.9	0.736	8.5583	8.9	0.745	8.5579	7.6	0.746
	±3	±8	±11	±3	±7	±13	±3	±6	±13
f_2	14.515	4.1	0.988	14.513	3.4	0.000	14.510	2.6	0.019
	±7	±8	±29	±8	±7	±34	±9	±6	±38
f_3	16.423	2.9	0.319	16.422	2.5	0.346	16.427	2.0	0.339
	±10	±8	±42	±11	±7	±45	±12	±6	±49
f_4	10.962	2.2	0.069	10.962	1.9	0.100	10.964	1.2	0.141
	±14	±8	±56	±15	±7	±60	±20	±6	±83
f_5	12.111	1.8	0.119	12.104	1.6	0.193	12.115	1.5	0.062
	±16	±8	±67	±17	±7	±71	±16	±6	±66

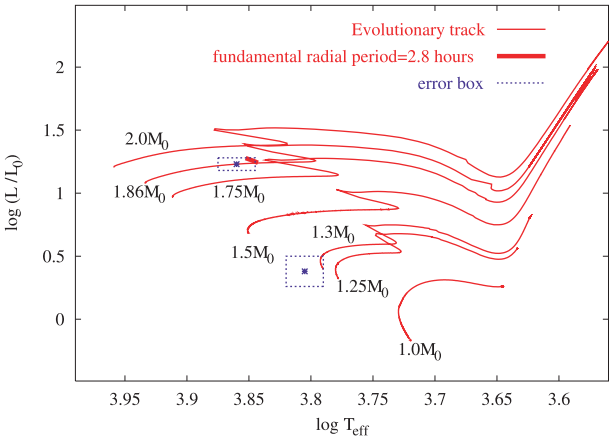

Fig. 5. Location of the two components together with the evolutionary tracks of Morel (1997) labeled in solar masses.

4. Discussion

4.1. Physical parameters

As indicated in Table 2, the eccentricity of the system is very low. Therefore, we can assume that circularisation is established, and in particular that the rotation angular frequency of each star is the same. If we subtract the binary motion from each component, we can derive projected rotation velocities of $v_1 \sin i = 73\,\mathrm{km\,s^{-1}}$ and $v_2 \sin i = 36\,\mathrm{km\,s^{-1}}$ for HD 173977 and its companion, respectively. From the angular frequency of the system, we can estimate a projected radius of $2.6\,R_\odot$ for the main component and $1.3\,R_\odot$ for its companion. The spectral type of the system provided in the literature is F2 (CDS) or F1 (Fekel et al. 2003). Unfortunately, our spectral domain is not convenient to determine precisely the spectral characteristics of the two components. Since the mass ratio is $M_1/M_2 = 1.45$, the spectral type associated with the primary is slightly hotter than F1. If we suppose an F0 spectral type for the primary, and using standard calibrations and Hipparcos distances, we obtain $\log(T_{\rm eff}) = 3.86 \pm 0.015$ and $\log(L/L_\odot) = 1.23 \pm 0.05$ for the system. We have calculated the evolutionary tracks shown in Fig. 5 using the CESAM code (Morel 1997). The best solution for the system is presented in Table 6. Using the 2 masses displayed in Table 6, we derived an inclination of $i = 67°$.

Table 6. Parameters for the two components as provided by the evolutionary tracks of Morel (1997). Data are compatible for a coeval evolution age of 1.13 Gy.

	Component 1	Component 2
$M\ [M_\odot]$	1.87	1.30
$R\ [R_\odot]$	2.87	1.42
$\mathrm{Log}(T_{\rm eff})$	3.84	3.80
$\log(L/L_\odot)$	1.26	0.42

In order to improve the above parameters, we used an independant approach based on the behaviour of light curves in a close binary system. The fits to the light curves were run using an improved version of the Wilson-Devinney (W-D) program (Wilson & Devinney 1971) that includes a model atmosphere routine developed by Milone et al. (1992) for the computation of the stellar radiative parameters. The W-D program is physically realistic with the stars in the binary system being modelled as Roche equipotential surfaces. Both reflection and proximity effects are taken into account. Initial test runs indicated a binary in a detached configuration and the W-D program mode was set accordingly in all subsequent runs. The bolometric albedo and gravity-brightening coefficients were set to 1 for both components. For the limb darkening, we used a logarithmic law as defined in Klinglesmith & Sobieski (1970). The mass ratio was adopted from the spectroscopic solution in Table 2. Again, both primary and secondary components were assumed to rotate synchronously.

Our preferred solution yields an inclination of $i = 60 \pm 2°$, a gravitational potential for the primary star of $\Omega_1 = 3.37 \pm 0.03$, and a phase offset (with respect to the ephemeris in Table 2) of 0.661 ± 0.003. Equivalently, the mean relative radius (i.e., $r \equiv R/a$) of the primary results in a value of $r_{\rm m} = 0.386 \pm 0.006$. A graphical illustration of the fits to the *vby* light curves is presented in Fig. 6, with r.m.s. residuals of 0.008 mag, 0.007 mag, and 0.006 mag, for v, b, and y, respectively.

As can be seen, the main discrepancy between these 2 independant methods concerns the inclination angle, which is between $i = 60°$ and 67°, a relatively small range. Nevertheless,

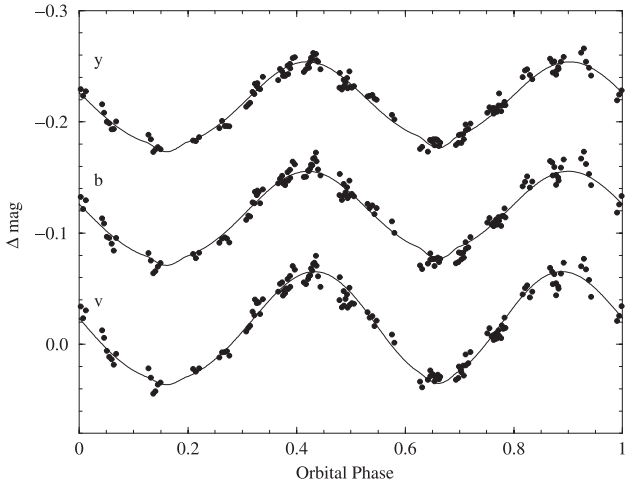

Fig. 6. Light curves and corresponding fits using the Wilson & Devinney (1971) method.

we point out the need for new spectroscopic observations with a wider wavelength domain to define the spectral type of both components.

4.2. Pulsation

The calculated evolutionary tracks shown in Fig. 5, using the CESAM code (Morel 1997), is also used to compute the pulsational characteristics of each stellar model. The primary component is clearly located inside the lower part of the instability strip and it is expected that the star shows the typical mix of radial and non-radial pulsations of δ Scuti stars (Breger & Montgomery 2000). Conversely, the secondary is outside this instability strip, so pulsation cannot originate from it. The secondary is also too red to be in the instability strip of the γ Doradus stars (Warner et al. 2003). The colour solution given in Table 5 is not precise enough to discriminate between radial ($\ell = 0$) and dipolar ($\ell = 1$) modes for the first frequency, but if we assume that f_1 is a radial mode then we can select a series of stellar models (indicated by a solid line inside the error box) that matches the 2.8 hour observed period. The masses of these models range from 1.87 to 1.90 $M_\odot$. For all these models, non-adiabatic theoretical calculations predict overstable modes from $Q = 0.06\,\mathrm{d}$ ($f = 4.6\,\mathrm{d}^{-1}$) to $Q = 0.0115\,\mathrm{d}$ ($f = 25.3\,\mathrm{d}^{-1}$), a range in which all the observed frequencies are found. All the models along the line of constant period match the first 4 radial overtones, at a few percent error, with 4 of the 5 observed frequencies shown in Table 5. In this region of the instability strip the number of theoretically excited low order modes ($\ell = 0$, 1, 2 and 3) for this frequency range is very large (around 50). Particularly, one of the models plotted in the line at constant period predicts $F = 2.80\,\mathrm{h}$ ($8.57\,\mathrm{d}^{-1}$), $1H = 2.15\,\mathrm{h}$ ($11.16\,\mathrm{d}^{-1}$), $2H = 1.72\,\mathrm{h}$ ($13.95\,\mathrm{d}^{-1}$) and $3H = 1.42\,\mathrm{h}$ ($16.90\,\mathrm{d}^{-1}$). If one admits that f_1 is associated with a radial mode, f_2 is then close to the theoretical $2H$ value and f_3 is close to that of $3H$. One of the two possible frequencies for f_4 is next to the $1H$ value, and finally the last one f_5 is between $1H$ and $2H$. However, in this framework, the differences between theoretical and measured values for f_2, f_3 and f_4 are well above the observational error bars. This implies that either we are not dealing with radial modes, nor the observed frequencies are different from the theoretical values for reasons that could be linked, for instance, to evolutionary status or binarity.

5. Conclusion

From new spectroscopic and photometric observations, we show that HD 173977 is an SB2 star in a circular orbit. The pulsation spectrum shows typical δ Scuti star frequencies, hence HD 173977 cannot be considered as a γ Doradus star, the low frequency detected in Hipparcos data being due to geometrical variations.

From two independant methods, evolutionary tracks and light variations, we were able to compute the physical parameters of both components.

It is extremely important to note that, within the observational errors, the masses, radii, effective temperatures, luminosities and other physical quantities derived from binary motions, evolutionary tracks and asteroseismic considerations are almost the same. The system is therefore very interesting for a detailed asteroseismic study deserving more dedicated and precise observations to possibly deduce details on the internal structure of the primary component.

Acknowledgements. The authors are much indebted to the referee, Dr. G. Handler, for his constructive criticism on an earlier version of the paper, which helped them to make significant improvements to the study. R.G. and A.M. acknowledge financial support from the program ESP2001-4528-PE. The authors thank also the CNRS-CONACYT agreement for support.

References

Breger, M., & Montgomery, M. 2000, Delta Scuti and Related Stars, ASP Conf. Ser., 410
ESA 1997, The Hipparcos and Tycho catalogues, ESA SP-1200
Fekel, F. C., Warner, P. B., & Kaye, A. B. 2003, AJ, 125, 2196
Handler, G. 1999, MNRAS, 309, L19
Klinglesmith, D. A., & Sobieski, S. 1970, AJ, 75, 175
Mathias, P., Le Contel, J.-M., Chapellier, E., et al. 2004, A&A, 417, 189
Milone, E. F., Stagg, C. R., & Kurucz, R. L. 1992, ApJS, 79, 123
Montgomery, M. H., & O'Donoghue, D. 1999, Delta Scuti Newsletter, 13, 28
Morel, P. 1997, A&A, 124, 597
Rodriguez, E., & Breger, M. 2001, A&A, 366, 178
Scargle, J. D. 1998, ApJ, 263, 835
Sperl, M. 1998, Comm. Astroseismol., 111, 1
Vanicek, P. 1971, Ap&SS, 12, 10
Warner, P. B., Kaye, A. B., & Guzik, J. A. 2003, ApJ, 593, 1049
Wilson, R. E., & Devinney, E. J. 1971, ApJ, 166, 605 (W-D)